Available online at www.sciencedirect.com

SCIENCE DIRECT®

Inorganica Chimica Acta 358 (2005) 1798–1806

Inorganica Chimica Acta

www.elsevier.com/locate/ica

Substitution and redox reactions of mono- and dinuclear ruthenium complexes containing the $pyN_2H_2S_2^{2-}$ ligand [$pyN_2H_2S_2^{2-}$ = 2,6-bis(2-mercaptophenylaminomethyl)pyridine(2−)] ☆

D. Sellmann †, S.Y. Shaban *, A. Rösler, F.W. Heinemann

Institut für Anorganische Chemie der Universität Erlangen-Nürnberg, Egerlandstraße 1, D-91058 Erlangen, Germany

Received 14 May 2004; accepted 12 December 2004

Abstract

In quest of ruthenium complexes having [RuN_3S_2] cores, a non-flexible configuration, *trans*-thiolate donors and exchangeable coligand L, [Ru(L)($pyN_2H_2S_2$)] complexes have been synthesized [$pyN_2H_2S_2^{2-}$ = 2,6-bis(2-mercaptophenylaminomethyl) pyridine (2−)]. Treatment of [$RuCl_2(CH_3CN)_4$] with $pyN_2H_2S_2^{2-}$ gave [Ru(py)($pyN_2H_2S_2$)] (**1**). The pyridine coligand in **1** proved to be labile and could be substituted by either CO or DMSO under normal conditions to give [Ru(CO)($pyN_2H_2S_2$)] (**2**) and [Ru(DMSO)($pyN_2H_2S_2$)] (**3**), respectively. Alternatively, **2** could be obtained directly from [$RuCl_2(CH_3CN)_4$] and $pyN_2H_2S_2^{2-}$in the presence of CO, whereas the reaction in the absence of CO gave the dinuclear [$Ru(pyN_2H_2S_2)]_2$ (**8**). Treatment of either **2** or **3** with $NOBF_4$ afforded [Ru^{III}(CO)($pyN_2H_2S_2$)]BF_4 ([**4**]BF_4) and [Ru(NO)($pyN_2H_2S_2$)]BF_4 ([**5**]BF_4), respectively. Treatment of [**5**]BF_4 with either NEt_4N_3 or N_2H_4 afforded the amide [Ru(NO)(pyN_2HS_2)] (**6**) and the hydrazine [$Ru(N_2H_4)(pyN_2H_2S_2)$] (**7**), respectively. Treatment of the dinuclear **8** with either one or two equivalents of $NOBF_4$ afforded the mixed-valence diruthenium (II,III) [$Ru^{III}Ru^{II}(pyN_2H_2S_2)_2$]$BF_4$ ([**9**]BF_4) and the diruthenium (III) [$Ru^{III}Ru^{III}(pyN_2H_2S_2)_2$]$(BF_4)_2$ {[**10**]$(BF_4)_2$}, respectively. The diruthenium (III) complex [**10**]$(BF_4)_2$ is diamagnetic, which can be ascribed to spin–spin pairing between the two Ru^{III} atoms. A preliminary structure determination of [**10**]$(BF_4)_2$ supports this observation, indicating a single bond between the two Ru^{III} atoms. Novel diruthenium complex of this type could be synthesized more generally by treatment of [$RuCl_3(MeSPh)_3$] with $pyN_2H_2S_2^{2-}$. All complexes were characterized by spectroscopic methods and elemental analysis. The cations [**9**]$^+$ and [**10**]$^{2+}$ were characterized by X-ray structure analysis.

Keywords: Spin–spin pairing; Ru–Ru single bond; Oxidation; Labile coligand

1. Introduction

Structure–function relationships of transition metal complexes are primarily determined by the metal oxidation state, type and number of the ligand donor atoms, and the structure of the metal ligand core [1]. In quest of metal complexes that combine both structural (metal sulfur sites) and functional (reactivity) features of nitrogenase centers, our interest focuses on complexes with multidentate ligands which contain amine N, thioether S, and thiolate S donors. Important requirements for the activation of N_2 by nitrogenases are considered to be electron-rich metal centers [2] as well as a *trans*-coordination of the thiolate donors [3]. In order to meet these requirements, we have developed the [Ru($pyN_2H_2S_2$)] fragment [4]. This fragment was

---

☆ Transition metal complexes with sulfur ligands 166. Part 165: D. Sellmann, K. Hein, F.W. Heinemann, *Inorg. Chim. Acta*, 2004, in press.

* Corresponding author. Tel.: +49 9131 8527782; fax: +49 9131 8527367.

E-mail address: shaban@anorganik.chemie.uni-erlangen.de (S.Y. Shaban).

† Deceased.

0020-1693/$ - see front matter © 2004 Elsevier B.V. All rights reserved.
doi:10.1016/j.ica.2004.12.004

found to bind as yet CO, DMSO and PPh_3. The resulting complexes exhibit the thiolate and the amine donors to be in *trans*-position as well as a high electron density at the ruthenium centers, as evidenced by the ν(CO) frequency of [Ru(CO)($pyN_2H_2S_2$)] (1927 cm^{-1}) [4] but all complexes [Ru(L)($pyN_2H_2S_2$)] (L = CO, DMSO, PPh_3) synthesized so far are extremely substitution inert. For example, the synthesis of [Ru(CO)($pyN_2H_2S_2$)] from [Ru(DMSO)($pyN_2H_2S_2$)] requires 120 °C and 140 bar. Herein, we describe our efforts to synthesize [Ru(L)($pyN_2H_2S_2$)] complexes with labile coligand L, which may be substituted by nitrogenase-relevant small molecules. The exchange of L proved to be the major problem. In the course of our investigations, we have isolated a diamagnetic thiolate-bridged dinuclear [$Ru^{III}Ru^{III}$($pyN_2H_2S_2$)$_2$](BF_4) {[**10**](BF_4)$_2$} exhibiting spin–spin pairing as well as a single bond between the two Ru^{III} centers. Few examples of thiolate-bridged $Ru^{III}Ru^{III}$ of this type are known, and most of these are limited to complexes containing either Cp* [5] or other bridging ligands (RCO_2^-, OH^-, and dppm/Cl^-) [6] in the coordination sphere.

2. Results and discussion

2.1. Synthesis and reactions of the complexes

Scheme 1 summarizes the syntheses and reactions of [Ru($pyN_2H_2S_2$)] complexes.

Treatment of [$RuCl_2(py)_4$] with $pyN_2H_2S_2$–H_2 in the presence of two equivalents of LiOMe (for deprotonation of the thiol S–H functions) afforded a red [Ru(py)($pyN_2H_2S_2$)] (**1**). The pyridine coligand in complex **1** proved to be labile and could be replaced by either CO or DMSO at room temperature to afford [Ru(CO)($pyN_2H_2S_2$)] (**2**) and [Ru(DMSO)($pyN_2H_2S_2$)] (**3**), respectively. Alternatively, complex **2** could be obtained from [$RuCl_2(py)_4$] and $pyN_2H_2S_2$–Li_2 in the presence of an excess of CO at 65 °C. Complex **2** exhibits a ν(CO) frequency at 1927 cm^{-1} in KBr indicating a high electron density at the metal center and a strong Ru–CO bond, and solid **2** is indeed stable at room temperature over prolonged periods of time. Complex **3** proved also substitution inert towards CO, N_2H_4, N_2 or NO ligands. It could not be reacted with CO at room temperature at pressures ranging from 1 to 100 bar. Only under very drastic conditions in an autoclave (140 bar CO, 120 °C), a slow reaction took place to give complex **2** [4].

In attempts to diminish the substitution inertness, complexes **2** and **3** were treated with $NOBF_4$. On addition of $NOBF_4$ to a yellow CH_2Cl_2 suspension of **2** at 0 °C, a brown suspension was obtained, from which a brown product was isolated and fully characterized as [Ru(CO)($pyN_2H_2S_2$)]BF_4 ([**4**]BF_4) in which the ruthenium (II) was oxidized to ruthenium (III). Complex [**4**]BF_4 proved as substitution inert as the precursor **2**. For example, treatment of [**4**]BF_4 with $NaBH_4$ yielded **2** and showed that the ruthenium oxidation is reversible. In accordance with expectations,

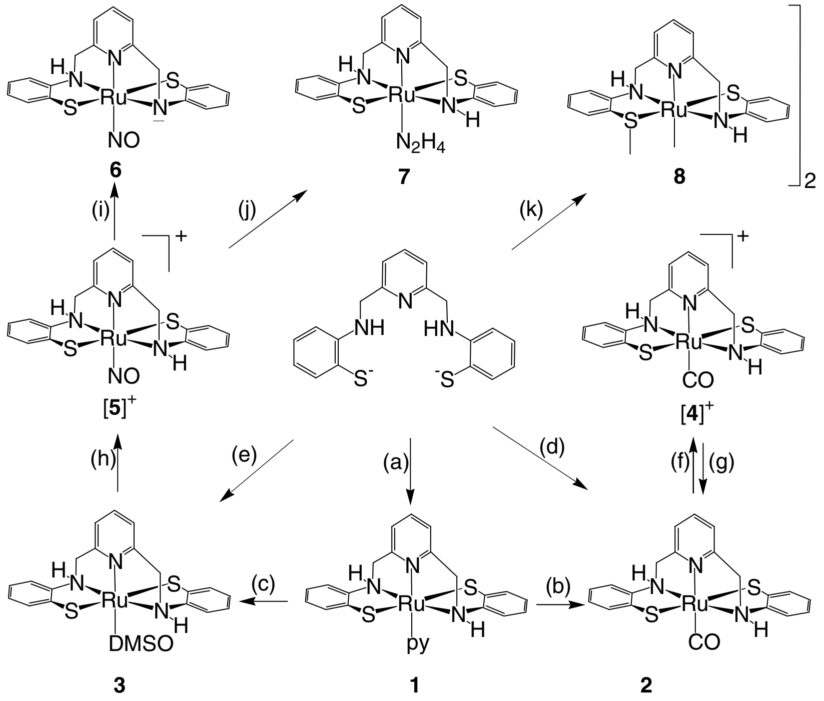

Scheme 1. Syntheses and reactions of [Ru($pyN_2H_2S_2$)] complexes: (a) +[$RuCl_2(py)_4$]/MeOH/65 °C; (b) +CO/THF/20 °C; (c) +exc. DMSO/20 °C; (d) +[$RuCl_2(CH_3CN)_4$]/CO/MeOH/65 °C; (e) +[$RuCl_2(DMSO)_4$]/THF/65 °C; (f) +$NOBF_4$/CH_2Cl_2/20 °C; (g) +$NaBH_4$/MeOH/20 °C; (h) +$NOBF_4$/CH_2Cl_2/20 °C; (i) +NEt_4N_3/MeOH/20 °C; (j) +N_2H_4/THF/20 °C; (k) +[$RuCl_2(CH_3CN)_4$]/MeOH/65 °C.

the oxidation of **2** to yield [**4**]BF_4 shifts the ν(CO) band to higher frequency (∼50 cm^{-1}).

The redox interconversion of **2** and [**4**]BF_4 was also achieved electrochemically. The cyclic voltammogram of **2** exhibits two simple successive redox processes. No reduction waves were observed within the solvent limits. Thus, the redox process observed at $E_{1/2}$ = +332 mV is assignable to the Ru^{II}/Ru^{III} couple (**2**/[**4**]BF_4), whereas the other at $E_{1/2}$ = +737 mV results from the Ru^{III}/Ru^{IV} couple. The most remarkable feature is the relatively large separation between the two redox potentials (∼400 mV), implying that the Ru^{III} complex [**4**]BF_4 is fairly stable.

When a CH_2Cl_2 suspension of [Ru(DMSO)($pyN_2H_2S_2$)] (**3**) was treated with an equimolar amount of $NOBF_4$, a brown [Ru(NO)($pyN_2H_2S_2$)]BF_4 ([**5**]BF_4) was produced. It was surprising to observe such reaction of **3** with $NOBF_4$ under normal conditions. However, complex [**5**]BF_4 showed a ν(NO) frequency at 1858 cm^{-1} in KBr and 1870 cm^{-1} in MeOH and this made the cation [**5**]$^+$ a candidate for attempts to convert the NO into N_2 ligand by addition of nitrogen nucleophiles to the nitrosyl N atom [7]. For this reason, complex [**5**]BF_4 was treated with NEt_4N_3 and N_2H_4.

Addition of an equimolar amount of NEt_4N_3 to a brown suspension of [**5**]BF_4 in MeOH yielded gray, sparingly soluble product whose elemental analysis and spectroscopic data were compatible with those for [Ru(NO)(pyN_2HS_2)] (**6**) with one amide donor. The formation of the amide could further be substantiated by protonation of neutral **6** with HBF_4 to afford isomerically pure [**5**]BF_4. The deprotonation is accompanied by a shift of the ν(N=O) frequency (KBr) from 1858 cm^{-1} in [**5**]BF_4 to 1801 cm^{-1} in **6**. The N–H Broensted acidity could further be established by a H^+/D^+ exchange reaction. Addition of D_2O to a DMF solution of [**5**]BF_4 spontaneously afforded [Ru(NO)(pyN_2HDS_2)] as shown by the following equation:

$$[Ru(NO)(pyN_2H_2S_2)]^+ \rightleftarrows [Ru(NO)(pyN_2HS_2)] + H^+ \tag{1}$$

The Broensted acidity was observed only for the nitrosyl complex [**5**]BF_4 as expected from the ^1H NMR chemical shift of the NH protons (δ 10.5 ppm), which is deshielded relative to the ca. δ 7.9 ppm shifts of the other complexes. One possible reason for that could be the positive charge of the cation [**5**]$^+$, which facilitates proton loss from the NH leading to amide formation. The limited amide formation of [Ru($pyN_2H_2S_2$)] fragments compared to that of [Ru($N_2H_2S_3$)] [8] and [Ru($N_3H_3S_2$)] [9] fragments could be a consequence of the core structures of [Ru ($pyN_2H_2S_2$)] complexes that are expected to disfavor the deprotonation of the aromatic N–H function into amide function, as it requires a conversion of tetrahedral four-coordinate N into planar three coordinate or distorted tetrahedral N atoms [10] and this could further explain why the protonation of **6** gave [**5**]BF_4 in only one isomer.

When a brown THF suspension of [**5**]BF_4 was treated with excess of anhydrous N_2H_4, gas was evolved and a red-brown solid was formed, which exhibits a strong band in its IR (KBr) spectrum at around 2037 cm^{-1}, consistent with the formation of a bound azide complex. However, this product was so insoluble in all common solvents that it could not be adequately characterized. An orange solid was formed upon addition of ether to the filtrate, which was isolated and characterized as hydrazine complex [Ru(N_2H_4)($pyN_2H_2S_2$)] (**7**). Complex **7** demonstrates that the [Ru($pyN_2H_2S_2$)] fragment can bind “hard” σ coligands. However, **7** proved too labile to be used as a starting material. All efforts to oxidize **7** or to get a N_2 species by the reaction of N_2 with **7** remained as yet unsuccessful, instead dinuclear [{Ru($pyN_2H_2S_2$)}$_2$] (**8**) was formed.

The dinuclear **8** was found not to react with boiling DMSO, pyridine, or with CO in these solvents. In attempts to diminish the inertness, the dinuclear **8** was treated with different oxidizing agents (see Scheme 2).

Treatment of **8** with one equivalent of $NOBF_4$ in CH_2Cl_2 afforded the mixed-valence diruthenium (II,III) [$Ru^{II}Ru^{III}$($pyN_2H_2S_2$)$_2$]BF_4 ([**9**]BF_4). While treatment of **8** with two equivalents of $NOBF_4$ afforded the diruthenium (III) [$Ru^{III}Ru^{III}$($pyN_2H_2S_2$)$_2$](BF_4)$_2$ ([**10**](BF_4)$_2$). The ^1H NMR spectroscopy supports the diamagnetic nature of [**10**](BF_4)$_2$, in which the chemical shifts are within the normal diamagnetic range (1–10 pm). The diamagnetic character of [**10**](BF_4)$_2$ can be ascribed to the spin–spin pairing between the two Ru^{III} centers. The preliminary structure of [**10**](BF_4)$_2$

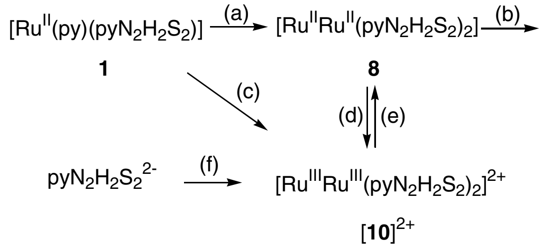

Scheme 2. Syntheses and reactions of [{Ru($pyN_2H_2S_2$)}$_2$]$^{x+}$ complexes (x = 0, 1.2): (a) +N_2H_4/THF/65 °C; (b) +$NOBF_4$/CH_2Cl_2/20 °C; (c) +2$NOBF_4$/CH_2Cl_2/20 °C; (d) +2$NOBF_4$ or I_2/CH_2Cl_2/20 °C; (e) +$NaBH_4$/DMSO/20 °C; (f) +[Ru(Cl)$_3$(MeSPh)$_3$]/THF/MeOH/65 °C.

was also confirmed by X-ray structure analysis which shows Ru(III)–Ru(III) single bond distance (280.6(2) pm), consistent with reported values for Ru–Ru single bonds (260–290 pm) [11]. In an alternative way, the cation $[\mathbf{10}]^{2+}$ could be synthesized more generally by either treatment of $[Ru(Cl)_3(MeSPh)_3]$ with $pyN_2H_2S_2{}^{2-}$ or treatment of **8** with I_2. The electrochemistry of $[\mathbf{10}](BF_4)_2$ was studied by cyclic voltammetry. Only one reduction process was observed within the solvent limit at $E_{1/2} = -438$ mV, which is assignable to the $Ru^{III}Ru^{III}/Ru^{II}Ru^{III}$ couple ($[\mathbf{10}]^{2+}/[\mathbf{9}]^+$). No oxidation waves were observed within the solvent limits. The most remarkable feature is the high potential of the $Ru^{III}Ru^{III}/Ru^{II}Ru^{III}$ couple as well as the absence of a further reduction process $Ru^{II}Ru^{III}/Ru^{II}Ru^{II}$ couple, indicating that the $Ru^{II}Ru^{III}$ complex $[\mathbf{9}]BF_4$ is fairly stable.

2.2. Characterization and general properties of the complexes

As far as possible, all complexes have been characterized by common spectroscopic methods and by elemental analysis. All mononuclear complexes **2**, **3**, $[\mathbf{4}]BF_4$, $[\mathbf{5}]BF_4$, **6** and **7** as well as the dinuclear $[\mathbf{9}]BF_4$ and $[\mathbf{10}](BF_4)_2$ show moderate solubility in DMF and DMSO, while complex **1** is soluble only in pyridine and dinuclear **8** was found to be insoluble in all common solvents. Consequentially, no NMR spectra of **8** could be recorded and this complex could be only characterized by its IR and mass spectra and elemental analysis. The IR spectra in KBr show weak ν(N–H) bands in the range from 3284 to 3140 cm^{-1}, besides the characteristic bands of the coligands. For example, strong ν(CO) absorption bands at 1927 and 1975 cm^{-1} characterize complexes **2** and $[\mathbf{4}]BF_4$, respectively. Strong ν(NO) bands at 1858 and 1801 cm^{-1} characterize the nitrosyl complexes $[\mathbf{5}]BF_4$ and **6**, respectively. Characteristic strong ν(B–F) bands are seen for $[\mathbf{4}]BF_4$ (1083 cm^{-1}), $[\mathbf{5}]BF_4$ (1064 cm^{-1}), $[\mathbf{9}]BF_4$ (1069 cm^{-1}) and $[\mathbf{10}](BF_4)_2$ (1074 cm^{-1}), respectively.

The FD mass spectra exhibit either peaks for the molecular ions or ions resulting from loss of the coligands. The $^{13}C\{^1H\}$ NMR spectra proved the most suitable spectroscopic probe for determining the symmetry of the complexes. Nine plus one ^{13}C NMR signals for the aromatic and the methylene C atoms of the chelate ligands clearly indicate C_2-symmetry for all mononuclear complexes.

The ^1H NMR spectrum of $[\mathbf{10}](BF_4)_2$ supports the diamagnetic nature of structure $[\mathbf{10}](BF_4)_2$, indicating spin–spin pairing between the two Ru^{III} centers. The chemical shifts are within the normal diamagnetic range (0–10 ppm). Seventeen and two ^{13}C NMR signals for the aromatic and the methylene C atoms for $[\mathbf{10}](BF_4)_2$ indicate C_1-symmetry. The ^1H NMR spectra, too, are consistent with C_2-symmetry for all mononuclear complexes and C_1-symmetry for $[\mathbf{10}](BF_4)_2$. For example, the chemically equivalent CH_2 protons of the free ligand become magnetically nonequivalent in all mononuclear complexes giving rise to two doublets and the lower field doublet further splits into a doublet of doublets due to coupling with the adjacent NH proton. For $[\mathbf{10}](BF_4)_2$, the methylene protons are appearing as two doublets and two doublets of doublets in the low field, indicating C_1-symmetry (Fig. 1).

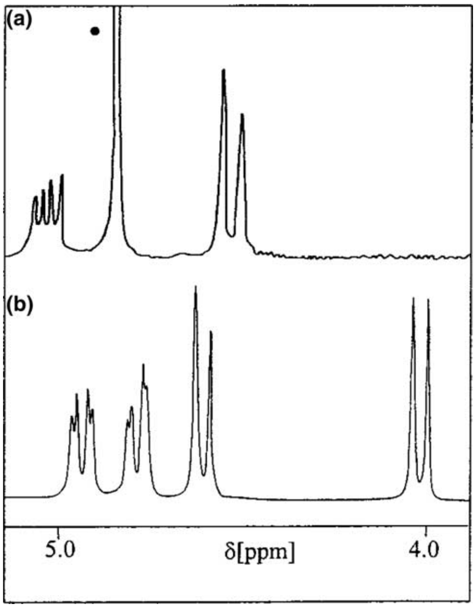

Fig. 1. The CH_2 region in ^1H NMR of: (a) **1** in pyridine-d_5(• = H_2O in pyridine-d_5); (b) $[\mathbf{10}](BF_4)_2$ in DMSO-d_6.

2.3. X-Ray structure determination of $[\{Ru(pyN_2H_2S_2)\}_2]Cl \cdot 4MeOH$ ($[\mathbf{9}]Cl \cdot 4MeOH$) and $[\{Ru(pyN_2H_2S_2)\}_2](BF_4)_2 \cdot 2DMSO \cdot$ acetone $\cdot$ n-hexane ($[\mathbf{10}](BF_4)_2 \cdot 2DMSO \cdot$ acetone $\cdot$ n-hexane)

The structure of $[Ru(pyN_2H_2S_2)]_2Cl \cdot 4MeOH$ ($[\mathbf{9}]Cl \cdot 4MeOH$) and a preliminary structure of $[\{Ru(pyN_2H_2S_2)\}_2](BF_4)_2 \cdot 2DMSO \cdot$ acetone $\cdot$ *n*-hexane ($[\mathbf{10}](BF_4)_2 \cdot 2DMSO \cdot$ acetone $\cdot$ *n*-hexane) were determined by X-ray crystallography. $[\mathbf{10}](BF_4)_2$ proved to be very difficult to obtain suitable single crystals. A number of structure determinations attempted so far resulted always in high residual electron density maxima close to the two central ruthenium atoms and showed the presence of numerous solvent molecules. However, the overall connectivity and geometry of $[\mathbf{10}](BF_4)_2$ could be established (Fig. 3).

Selected bond distances and angles are listed in Table 1. Complexes $[\mathbf{9}]Cl$ and $[\mathbf{10}](BF_4)_2$ contain two C_2-symmetrical $[Ru(pyN_2H_2S_2)]$ units which are coupled through thiolate bridges. Each Ru atom is pseudo-octahedrally coordinated by three S and three N donor atoms. The two thiolate as well as the two amine donors

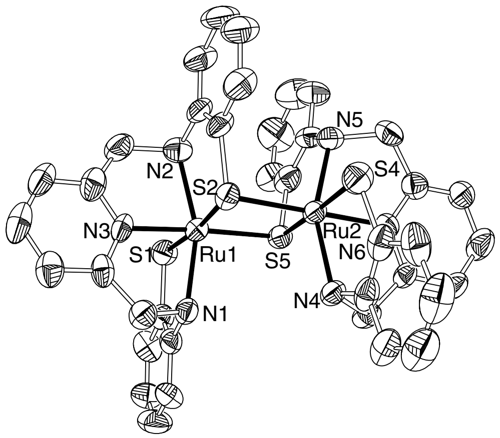

Fig. 2. Molecular structure of the cation of $[\{Ru(pyN_2H_2S_2)\}_2]Cl \cdot 4MeOH$ ($[\mathbf{9}]Cl \cdot 4MeOH$) (50% probability ellipsoids, C-bound H atoms, anions and solvents omitted).

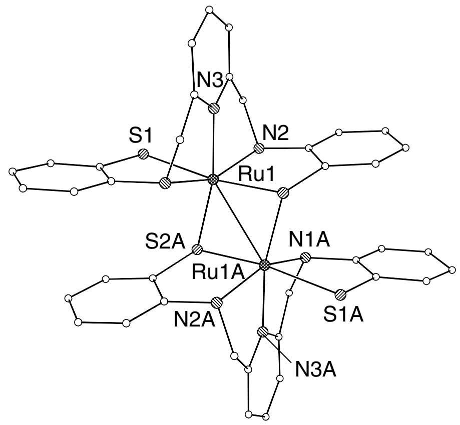

Fig. 3. The overall connectivity and geometry of the cation $[\mathbf{10}]^{2+} \cdot 2DMSO \cdot acetone \cdot n\text{-hexane}$, as obtained from a preliminary X-ray structure determination.

of the $pyN_2H_2S_2$ ligand occupy pairwise *trans*-positions, thus proving the steric rigidity of the $py(CH_2)_2$ backbone. The monocation $[\{Ru(pyN_2H_2S_2)\}_2]^+$ contains two homochiral centers which are rotated against each other by 84.2° and the dimeric complex thus possesses C_1-symmetry. Distances and angles show no anomalies. The Ru···Ru distance of $[\mathbf{9}]Cl \cdot 4MeOH$ [324.6(1) pm] does not indicate a Ru–Ru bonding interaction, while the Ru···Ru distance of $[\mathbf{10}](BF_4)_2 \cdot 2DMSO \cdot acetone \cdot n\text{-hexane}$ [280.6(2) pm] is in the range of the reported Ru–Ru single bonds (260–290 pm) [11]. The Ru–NH distances in $[\mathbf{9}]Cl \cdot 4MeOH$ (mean value ~ 216.3 (7) pm) are distinctly longer than the Ru–N (pyridine) distance (~202.0 (7) pm). It is also noted that the Ru1–S5 and Ru2–S2 distances (mean value 237.4 (2) pm) in the Ru–S(thiolate)–Ru bridges are of the same length as the Ru–S(thiolate) distances (mean value 236.3 (3) pm) within the two $[Ru(pyN_2H_2S_2)]$ halves. This certainly reflects the stability of this dinuclear complex towards dissociation into $[Ru(pyN_2H_2S_2)]$ monomers both in solution and in solid state (see Fig. 2).

Table 1
Selected bond distances and angles of $[\{Ru(pyN_2H_2S_2)\}_2]Cl \cdot 4MeOH$ ($[\mathbf{9}]Cl \cdot 4MeOH$) and $[\{Ru(pyN_2H_2S_2)\}_2](BF_4)_2 \cdot 2DMSO \cdot acetone \cdot n\text{-hexane}$ ($[\mathbf{10}](BF_4)_2 \cdot 2DMSO \cdot acetone \cdot n\text{-hexane}$)

Complex	$[\mathbf{9}]Cl \cdot 4MeOH$	$[\mathbf{10}](BF_4)_2 \cdot 2DMSO \cdot acetone \cdot n\text{-hexane}$[a]
Ru1–N1	217.8 (6)	216.2 (8)
Ru1–N2	217.8 (6)	216.9 (8)
Ru1–N3	202.0 (7)	204.8 (8)
Ru1–S1	234.7 (3)	240.2 (3)
Ru1–S2	237.2 (2)	229.7 (3)
Ru1–S5/S2A	237.5 (2)	231.4 (3)
Ru1–Ru1A/Ru2	324.6 (1)	280.6 (2)
N1–Ru1–S1	85.2 (2)	83.7 (2)
N2–Ru1–S1	90.5 (2)	95.2 (3)
N2–Ru1–S2	84.2 (2)	84.9 (3)
N3–Ru1–N1	78.8 (2)	79.0 (3)
N3–Ru1–S1	88.3 (2)	81.8 (3)
N3–Ru1–S5/S2A	177.6 (2)	166.2 (3)

[a] Preliminary data.

3. Conclusion

The results reported herein demonstrate that the $pyN_2H_2S_2^{2-}$ ligand forms ruthenium complexes possessing $[Ru(pyN_2H_2S_2)]$ cores that exhibit the desired configuration with thiolate donors in *trans*-position and that are structurally robust. The pyridine coligand in $[Ru(py)(pyN_2H_2S_2)]$ (**1**) was found to be labile and complex **1** can serve as a precursor for other complexes $[Ru(L)(pyN_2H_2S_2)]$ [L = CO (**2**), DMSO (**3**)]. The CO coligand in **2** was found to be substitution inert and could not be replaced by NO^+, instead oxidation occurred to give $[\mathbf{4}]BF_4$. The DMSO coligand in **3** could be replaced by NO^+ to give $[\mathbf{5}]BF_4$. Complex $[\mathbf{5}]BF_4$ showed reversible deprotonation of one amine NH function to give an amide donor ligand. The reaction of the nitrosyl complex $[\mathbf{5}]BF_4$ with N_2H_4 gave the hydrazine complex **7**, indicating that the $[Ru(pyN_2H_2S_2)]$ fragment can bind "hard" σ coligands.

In the course of our investigations, a series of thiolate-bridged diruthenium complexes $[Ru^{II}Ru^{II}(pyN_2H_2S_2)_2]$ (**8**), mixed-valence diruthenium (II,III) $[Ru^{II}Ru^{III}(pyN_2H_2S_2)_2]BF_4$ ($[\mathbf{9}]BF_4$) and diruthenium (III) $[Ru^{III}Ru^{III}(pyN_2H_2S_2)_2](BF_4)$ $\{[\mathbf{10}](BF_4)_2\}$ have been isolated and completely characterized. The diruthenium (III) $[\mathbf{10}](BF_4)_2$ is diamagnetic and the diamagnetic nature is assignable to a spin–spin pairing as well as a single bond between the two Ru^{III} centers. Few examples of thiolate-bridged $Ru^{III}Ru^{III}$ dimers possessing a spin–spin pairing as well as a single bond between the two Ru^{III} atoms exist, and these are limited to complexes containing Cp* in the coordination sphere [5]. $Ru^{III}Ru^{III}$ dimers of this type containing other bridging ligands

(RCO_2^-, OH^-, and dppm/Cl^-) have been reported [6], but only very few examples of a thiolato-bridged $Ru^{III}Ru^{III}$ dimeric complex that does not contain Cp* in the coordination sphere are known [5]. The first example of this type that does not contain Cp* in the coordination sphere has been reported by Cameron et al. [11]. Recently, an intermediate complex in the catalytic transformation of organic disulfides, $[Cp^*RuCl(\mu\text{-}SPh)]_2$, which also has a Ru^{III}–Ru^{III} single bond, has been isolated [12].

4. Experimental

4.1. General

Unless noted otherwise, all procedures were carried out under an atmosphere of N_2 using Schlenk techniques. Solvents were dried and distilled before use. As far as possible, reactions were monitored by IR or NMR spectroscopy. Spectra were recorded on the following instruments: IR (KBr discs or CaF_2 cuvettes, solvent bands were compensated): Perkin–Elmer 983, 1620 FT IR, and 16PC FT-IR; NMR: Jeol-JNM-GX 270, EX 270, and Lambda LA 400 with the protio-solvent signal used as an internal reference. Spectra were recorded at 25 °C; Mass spectra: Jeol MSTATION 700 spectrometers; Elemental analyses: Carlo Erba EA 1106 or 1108 analyzer; Cyclic voltammetry was performed with a Radiometer Copenhagen IMT 102 electrochemical interface using a three electrode cell with a glassy carbon (Radiometer Copenhagen EDI) working electrode and Pt reference and counter electrodes. Solutions were 10^{-3} M; $NBu_4[PF_6]$ (10^{-1} M) was used as the supporting electrolyte. Potentials were referenced to the normal hydrogen electrode (NHE) using Fc/Fc^+ as an internal standard $E(Fc/Fc^+) = +400$ mV versus NHE [13]. $[RuCl_2(CH_3CN)_4]$ [14], $[RuCl_2(py)_4]$ [15], $[Ru(Cl)_3(MeSPh)_3]$ [16] and $pyN_2H_2S_2$–H_2 [4] were prepared as described in the literature. Anhydrous hydrazine was obtained by twofold distillation of hydrazine hydrate over KOH under reduced pressure. LiOMe was purchased from Aldrich.

4.2. Syntheses

4.2.1. [Ru(py)($pyN_2H_2S_2$)] (**1**)

A suspension of $[Ru(Cl)_2(py)_4]$ (306 mg, 0.63 mmol) and $pyN_2H_2S_2$–Li_2 (230 mg, 0.63 mmol) in MeOH was heated at 65 °C for 3 h and stirred at 20 °C for 12 h. The resultant red solid was separated, washed with MeOH (10 ml) and dried in vacuo. Yield: 340 mg of $[Ru(py)(pyN_2H_2S_2)] \cdot 0.5MeOH$ (98%). ^1H NMR ([D_5]pyridine, 269.73 MHz): $\delta = 9.23$ (d, 2H, 2N*H*), 8.54 (d, $J_{HH} = 5.4$ Hz, 2H, H_α, pyridine), 8.00–7.94 (m, 2H, H_γ, pyridine), 7.73–7.62 (m, 2H, H_β, pyridine), 7.02–6.25 (m, 10H, $C_6H_4 + H_\beta$, pyridine), 5.15–5.05 (m, 2H, CH*H*), 4.62–450 (d, 2H, C*H*H_2). $^{13}C\{^1H\}$ NMR ([D_5]pyridine, 100.4 MHz): $\delta = 159.9$, 159.3, 155.3, 150.3, 149.5, 135.9, 132.7, 129.0, 126.9, 132.9, 120.5, 118.3 [C(aryl)], 69.4 (*C*H_2). IR (KBr): ν(tilde) = 3244 (w, N–H) cm^{-1}. MS (FD^+, pyridine): $m/z = 452$ $[Ru(pyN_2H_2S_2)]^+$. Calc. for $C_{24.5}H_{24}N_4O_{0.5}RuS_2$ (547.69): C, 53.73; H, 4.42; N, 10.22. Found: C, 53.41; H, 4.14; N, 10.05%.

4.2.2. [Ru(CO)($pyN_2H_2S_2$)] (**2**)

(a) From ***1***: CO gas was bubbled through a red suspension of **1** (100 mg, 0.19 mmol) in THF (25 ml) for 5 h in the course of which a yellow solid was precipitated, which was separated, washed with THF (20 ml) and CH_2Cl_2 (20 ml) and dried in vacuo. Yield: 80 mg of $[Ru(CO)(pyN_2H_2S_2)] \cdot 0.2CH_2Cl_2$ (85%). Calc. for $C_{20.2}H_{17.4}Cl_{0.4}N_3ORuS_2$ (497.57): C, 48.68; H, 3.68; N, 8.43; S, 12.87. Found: C, 48.78; H, 3.65; N, 8.44%.

(b) From $pyN_2H_2S_2$-H_2: At −78 °C, *n*-BuLi (0.34 ml, 0.85 mmol of 2.5 M solution in *n*-hexane) was added to a solution of $pyN_2H_2S_2$–H_2 (150 mg, 0.42 mmol) in THF (60 ml). After warming to room temperature, the solution was combined with a solution of $[Ru(Cl)_2(CH_3CN)_4]$ (143 mg, 0.42 mmol) in MeOH (30 ml) and heated at 65 °C under bubbling CO for 5 h. The resultant yellow solid was separated, washed with MeOH, THF, CH_2Cl_2 and Et_2O (each 10 ml) and dried in vacuo. Yield: 180 mg of $[Ru(CO)(pyN_2H_2S_2)] \cdot 0.2CH_2Cl_2$ (86%). ^1H NMR ([D_6]DMSO, 269.73 MHz): $\delta = 8.37$ (d, 2H, 2N*H*), 7.75 (t, $J_{HH} = 7.7$ Hz, 1H, H_γ, pyridine), 7.40 (d, $J_{HH} = 7.9$ Hz, 2H, H_β, pyridine), 7.14–7.11 (m, 4H, C_6H_4), 6.80–6.78 (m, 4H, C_6H_4), 4.84 (dd, 2H, C*H*H), 4.48 (d, 2H, CH*H*). $^{13}C\{^1H\}$ NMR ([D_6]DMSO, 100.4 MHz): $\delta = 207.2$ (*C*═O), 155.5, 149.9, 149.1, 137.3, 129.9, 126.1, 125.0, 120.5, 120.2 (*C*[aryl]), 69.2 (*C*H_2). IR (KBr): ν(tilde) = 3284 (w, N–H), 1927 (vs, C═O) cm^{-1}. MS (FD, DMSO): $m/z = 481$ $[Ru(CO)(pyN_2H_2S_2)]^+$. Calc. for $C_{20.2}H_{17.4}Cl_{0.4}N_3ORuS_2$ (497.57): C, 48.68; H, 3.68; N, 8.43; S, 12.87. Found: C, 48.81; H, 3.20; N; 8.75; S, 12.80%.

4.2.3. [Ru(DMSO)($pyN_2H_2S_2$)] (**3**)

A red solution of **1** (64 mg, 0.12 mmol) in DMSO (10 ml) was stirred for 48 h. The resulting yellow solution was concentrated to 5 ml and combined with THF (20 ml). The resulting yellow solid was isolated, washed with THF (20 ml), Et_2O (40 ml) and dried in vacuo. Yield: 54 mg of $[Ru(DMSO)(pyN_2H_2S_2)] \cdot DMSO$ (56%). ^1H NMR ([D_6]DMSO, 269.73 MHz): $\delta = 7.47$ (m, 3H, H_γ, pyridine + 2N*H*), 7.26–7.18 (m, 6H, Ar–*H*), 6.74–6.68 (m, 4H, Ar–*H*), 4.65(dd, 2H, C*H*H), 4.28 (d, 2H, CH*H*), 3.15 (s, 3H, *C*$H_3S(O)CH_3$), 2.75 (s, 3H, $CH_3S(O)C$*H_3*). $^{13}C\{^1H\}$ NMR ([D_6]DMSO, 100.4 MHz): $\delta = 156.78$, 150.54, 149.99, 134.3, 130.0, 125.7, 125.2, 119.7, 119.4 (*C*[aryl]), 68.7 (*C*H$_2$), 46.33, 44.20 (DMSO). IR (KBr): ν(tilde) = 3110 (w, N–H), 1012 (s, S=O) cm^{-1}. MS (FD, DMSO): *m*/*z* = 453 [Ru(pyN$_2$H$_2$S$_2$)]$^+$. Calc. for C$_{23}$H$_{29}$N$_3$ORuS$_4$ (592.83): C, 46.60; H, 4.93; N, 7.09; S, 21.64. Found: C, 46.45; H, 4.85; N, 7.00; S, 21.60%.

4.2.4. *[Ru(CO)(pyN$_2$H$_2$S$_2$)]BF$_4$ ([4]BF$_4$)*

At 0 °C, solid NOBF$_4$ (10 mg, 0.062 mmol) was added to a yellow suspension of **2** (30 mg, 0.062 mmol) in CH$_2$Cl$_2$ (10 ml). The reaction mixture was stirred at 0 °C for 4 h and at 20 °C for 30 min. The resultant brown solid was collected by filtration, washed with Et$_2$O (20 ml) and dried in vacuo. Yield: 25 mg of [Ru(CO)(pyN$_2$H$_2$S$_2$)]BF$_4$ · 0.5CH$_2$Cl$_2$ (70.64%). IR (KBr): ν(tilde) = 3240 (w, N–H), 1975 (vs, CO), 1083 (vs, B–F) cm^{-1}. MS (FD, CH$_2$Cl$_2$): *m*/*z* = 481 [Ru(CO)(pyN$_2$H$_2$S$_2$)]$^+$. Calc. for C$_{20.5}$H$_{18}$BClF$_4$N$_3$ORuS$_2$ (609.88): C, 40.37; H, 2.97; N, 6.90; S, 10.50. Found: C, 40.41; H, 2.96; N, 7.20; S, 10.71%.

4.2.5. *[Ru(NO)(pyN$_2$H$_2$S$_2$)]BF$_4$ ([5]BF$_4$)*

A mixture of NOBF$_4$ (73 mg, 0.62 mmol) and [Ru(DMSO)(pyN$_2$H$_2$S$_2$)] (330 mg, 0.62 mmol) in CH$_2$Cl$_2$ (20 ml) was stirred at 20 °C for 48 h. The resultant brown solid was separated by filtration, washed with CH$_2$Cl$_2$ (20 ml) and *n*-hexane (20 ml) and dried in vacuo. Yield: 290 mg of [Ru(NO)(pyN$_2$H$_2$S$_2$)] BF$_4$ · 1.5CH$_2$Cl$_2$ · 0.75*n*-hexane (61%). ^{1}H NMR ([D$_6$]DMSO, 269.73 MHz): δ = 10.57 (d, 2H, 2N*H*), 8.00 (t, J_{HH} = 7.7, 1H, H$_\gamma$, pyridine), 7.64 (d, J_{HH} = 7.7, 2H, H$_\beta$, pyridine), 7.42 (m, 2H, C$_6$*H*$_4$), 7.24 (m, 2H, C$_6$*H*$_4$), 7.08 (m, 4H, C$_6$*H*$_4$), 5.33 (dd, 2H, C*H*H), 4.94 (d, 2H, CH*H*). ^{13}C{^{1}H} NMR ([D$_6$]DMSO, 100.4 MHz): δ = 156.0, 147.9, 147.3, 141.78, 132.1, 129.1, 125.3, 124.1, 122.6 (*C*[aryl]), 69.5 (*C*H$_2$). IR (KBr): ν(tilde) = 3218 (w, N–H), 1858 (vs, NO), 1064 (vs, B–F) cm^{-1}. MS (FD, CH$_2$Cl$_2$): *m*/*z* = 483 [Ru(NO)(pyN$_2$H$_2$S$_2$)]$^+$. Calc. for C$_{25}$H$_{30.5}$BCl$_3$F$_4$N$_4$ORuS$_2$ (761.41): C, 39.44; H, 4.03; N, 7.36. Found: C, 39.53; H, 3.76; N, 7.56%.

4.2.6. *[Ru(NO)(pyN$_2$HS$_2$)] (**6**)*

A mixture of NEt$_4$N$_3$ (0.60 mg, 0.33 mmol) and [Ru(NO)(pyN$_2$H$_2$S$_2$)]BF$_4$ (185 mg, 0.33 mmol) in MeOH (20 ml) was stirred at 20 °C for 4 h in the course of which a gray solid was formed which was collected by filtration, washed with MeOH, H$_2$O and Et$_2$O (each 20 ml) and dried in vacuo. Yield: 100 mg [Ru(NO)(pyN$_2$HS$_2$)] · 2.5H$_2$O (64%). ^{1}H NMR ([D$_7$]DMF, 269.7 MHz): δ = 7.76 (t, 1H, *H*$_\gamma$, pyridine), 7.50 (d, 2H, C$_6$*H*$_4$), 7.19 (d, 4H, C$_6$*H*$_4$), 6.93 (t, 3H, C$_6$*H*$_4$), 6.80 (b, 1H, N*H*), 5.52 (d, 2H, C*H* H), 5.10 (d, 2H, CH*H*). IR (KBr) ν(tilde) = 1801 (vs, NO) cm^{-1}. MS (FD$^+$, CH$_2$Cl$_2$): *m*/*z* = 482 [Ru(NO)(pyN$_2$HS$_2$)]$^+$. Calc. for C$_{19}$H$_{21}$N$_4$RuO$_{2.5}$S$_2$ (536.60): C, 42.53; H, 3.25; N, 10.62; S, 12.15. Found C, 42.22; H, 3.40; N, 10.55; S, 12.61%.

4.2.7. *[Ru(N$_2$H$_4$)(pyN$_2$H$_2$S$_2$)] (7)*

A mixture of anhydrous N$_2$H$_4$ (0.5 ml, exc. 1.5 mmol) and [Ru(NO)(pyN$_2$H$_2$S$_2$)]BF$_4$ (250 mg, 0.44 mmol) in CH$_2$Cl$_2$ (15 ml) was stirred at 20 °C for 24 h. The resultant red-brown solid was removed by filtration. Subsequent addition of Et$_2$O (40 ml) to the filtrate led to the precipitation of an orange solid, which was separated, washed with MeOH (10 ml) and Et$_2$O (20 ml) and dried in vacuo. Yield: 38 mg of **7** · 1.8CH$_2$Cl$_2$ · CH$_3$CN (14%). ^{1}H NMR ([D$_6$]DMSO, 269.7 MHz): δ = 7.54 (m, 3H, 2N*H* + *H*$_\gamma$, pyridine), 7.32–7.26 (m, 5H, Ar–*H*), 6.78–6.72 (m, 5H, Ar–*H*), 4.91–4.86 (dd, 2H, C*H*H), 4.53–4.47 (d, 2H, CH*H*), 3.23 (s, 2H, NH$_2$), 2.13 (d, 2H, NH$_2$). ^{13}C{^{1}H} NMR ([D$_6$]DMSO, 100.4 MHz): δ = 157.44, 151.61, 150.47, 134.28, 130.69, 125.90, 125.27, 119.97, 119.55, (*C*[Aryl]), 69.1 (*C*H$_2$). IR (KBr): ν(tilde) = 3232, 3141 (w, N–H). MS (FD$^+$, CH$_2$Cl$_2$): *m*/*z* = 452 [Ru(pyN$_2$H$_2$S$_2$)]$^+$, 484 [Ru(N$_2$H$_4$)(pyN$_2$H$_2$S$_2$)]$^+$, 904 [{Ru(pyN$_2$H$_2$S$_2$)}$_2$]$^+$. Calc. for C$_{22.8}$H$_{27.6}$Cl$_{3.6}$N$_6$RuS$_2$ (679.97): C, 40.25; H, 4.09; N, 12.33. Found: C, 40.16; H, 4.16; N, 12.25%.

4.2.8. *[{Ru(pyN$_2$H$_2$S$_2$)}$_2$] (**8**)*

A yellow suspension of pyN$_2$H$_2$S$_2$-H$_2$ (284 mg, 0.8 mmol), LiOMe (1.6 ml, 1.6 mmol of 1 N solution in MeOH) and [Ru(Cl)$_2$(CH$_3$CN)$_4$] (270 mg, 0.8 mmol) in MeOH (30 ml) was heated at 65 °C for 3 h. The resulting fine red crystals were separated, washed with MeOH (20 ml) and Et$_2$O (30 ml) and dried in vacuo. Yield: 230 mg of **8** · MeOH (62%). IR (KBr): ν(tilde) = 3252, 3242 (w, N–H). MS (FD$^+$, DMSO): *m*/*z* = 904 [{Ru(pyN$_2$H$_2$S$_2$)}$_2$]$^+$. Calc. for C$_{39}$H$_{38}$N$_6$Oru$_2$S$_4$ (937.17): C, 49.98; H, 4.09; N, 8.97; S, 13.69. Found: C, 49.81; H, 3.82; N, 8.94; S, 13.54%.

4.2.9. *[Ru(pyN$_2$H$_2$S$_2$)]$_2$BF$_4$ ([**9**]BF$_4$)*

A red mixture of **8** (134 mg, 0.15 mmol) and NOBF$_4$ (17 mg, 0.15 mmol) in CH$_2$Cl$_2$ (25 ml) was stirred at −78 °C for 2 h and at 20 °C for 48 h in the course of which a green solid was precipitated, which was separated, washed with CH$_2$Cl$_2$ (20 ml) and *n*-hexane (10 ml) and dried in vacuo. Yield: 130 mg of [{Ru(pyN$_2$H$_2$S$_2$)}$_2$]BF$_4$ · CH$_2$Cl$_2$ (80%). IR (KBr): ν(tilde) = 3245, 3236 (w, N–H), 1069 (s, B–F). MS (FD$^+$, DMSO): *m*/*z* = 904 [{Ru(pyN$_2$H$_2$S$_2$)}$_2$]$^+$. Calc. for C$_{39}$H$_{36}$N$_6$BCl$_2$F$_4$Ru$_2$S$_4$ (1067.87): C, 43.50; H, 3.37; N, 7.80; S, 11.91. Found: C, 43.45; H, 3.46; N, 7.79; S, 11.93%.

4.2.10. *[{Ru(pyN$_2$H$_2$S$_2$)}$_2$](BF$_4$)$_2$ ([**10**](BF$_4$)$_2$)*

(a) From **1**. A mixture of **1** (100 mg, 0.19 mmol) and NOBF$_4$ (22 mg, 0.19 mmol) in CH$_2$Cl$_2$ (20 ml) was heated at 20 °C for 12 h. In the course of which a green

solid was precipitated, which was separated, washed with CH_2Cl_2 (20 ml) and *n*-hexane (10 ml) and dried in vacuo. Yield: 60 mg of [{Ru(py$N_2H_2S_2$)}$_2$] $(BF_4)_2$ (68%).

(*b*) *From* ***8***: A red suspension of **8** (156 mg, 0.17 mmol) and $NOBF_4$ (40 mg, 0.34 mmol) in CH_2Cl_2 (20 ml) was heated at 20 °C for 24 h. The resultant green solid was separated by filtration, washed with CH_2Cl_2 (20 ml) and *n*-hexane (10 ml), dried in vacuo and recrystallized from CH_2Cl_2/DMSO/*n*-hexane (10:1:10) to give a green solid. Yield: 110 mg of [**10**]$(BF_4)_2$ (60%). ^1H NMR ([D_6]DMSO, 269.7 MHz): $\delta = 7.97$ (t, $J_{HH} = 7.9$ Hz, 2H, H_γ, pyridine), 7.68 (d, 2H, N*H*), 7.61 (d, $J_{HH} = 7.7$ Hz, 2H, H_β, pyridine), 7.53 (d, $J_{HH} = 7.7$ Hz, 2H, H_β, pyridine), 7.40–5.90 (m, 16H, C_6H_4), 4.92 (dd, 2H, C*H*H), 4.83 (dd, 2H, CH*H*), 4.70 (d, 2H, C*H*H), 4.03 (d, H, CH*H*), 3.83 (d, 2H, N*H*). $^{13}C\{^1H\}$ NMR ([D_6]DMSO, 100.4 MHz): $\delta = 158.5$, 156.3, 146.8, 145.6, 141.1, 140.6, 139.8, 131.2, 130.1, 129.0, 127.5, 127.3, 126.2, 123.6, 123.0, 122.6, 122.0 (*C*[Aryl]), 70.61, 67.8 (*C*H_2). IR (KBr): ν(tilde) = 3234 (w, N–H), 1074 (vs, B–F). MS (FD^+, DMSO): *m*/*z* = 904 [{Ru(py$N_2H_2S_2$)}$_2$]$^+$. Calc. for $C_{38}H_{34}N_6B_2F_8Ru_2S_4$ (1078.74): C, 42.31; H, 3.18; N, 7.79. Found: C, 42.11; H, 3.26; N, 8.12%.

4.2.11. [{Ru(py$N_2H_2S_2$)}$_2$](Cl)$_2$ ([**10**](Cl)$_2$)

A suspension of py$N_2H_2S_2$-H_2 (355 mg, 1.0 mmol), LiOMe (2 ml, 2 mmol of 1 N solution in MeOH) and [Ru(Cl)$_3$(MeSPh)$_3$] (582 mg, 1.0 mmol) in MeOH/THF (each 30 ml) was heated at 65 °C for 4 h. The resulting fine green crystals were separated by filtration, washed with MeOH (20 ml) and ether (30 ml) and dried in vacuo. Yield: 130 mg of [**10**](Cl)$_2$ · MeOH (26%). IR (KBr): ν(tilde) = 3232 (w, N–H). MS (FD^+, DMSO): *m*/*z* = 904 [{Ru(py$N_2H_2S_2$)}$_2$]$^+$. Calc. for $C_{39}H_{38}N_6Cl_2$-ORu_2S_4 (1008.08): C, 46.47; H, 3.80; N, 8.34; S, 12.72. Found: C, 46.39; H, 3.77; N, 8.13; S, 12.62%.

4.2.12. [{Ru(py$N_2H_2S_2$)}$_2$](I)$_2$([**10**](I)$_2$)

A red suspension of **8** (100 mg, 0.11 mmol) and I_2 (28 mg, 0.11 mmol) in CH_2Cl_2 (20 ml) was stirred at 20 °C for 48 h in the course of which a green solid was precipitated, separated, washed with CH_2Cl_2 (10 ml) and *n*-hexane (10 ml) and dried in vacuo. Yield: 120 mg of [**10**](I)$_2$ · 0.5CH_2Cl_2 (91%). IR (KBr): ν(tilde) = 3241 (w, N–H). MS (FD^+, DMSO): *m*/*z* = 904 [{Ru(py$N_2H_2S_2$)}$_2$]$^+$. Calc. for $C_{38.5}H_{35}N_6ClI_2Ru_2S_4$ (120141): C, 38.49; H, 2.94; N, 6.70; S, 10.68. Found: C, 38.48; H, 3.13; N, 6.52; S, 10.48%.

4.3. X-ray structure analysis of [{Ru(py$N_2H_2S_2$)}$_2$]Cl · 4MeOH ([**9**]Cl · 4MeOH) and preliminary X-ray structure analysis of [{Ru(py$N_2H_2S_2$)}$_2$](BF$_4$)$_2$ · 2DMSO · acetone · n-hexane ([**10**](BF$_4$)$_2$ · 2DMSO · acetone · n-hexane)

Black block-shaped single crystals of [**9**]Cl · 4MeOH were grown at room temperature by slow air diffusion of a solution of [{Ru(py$N_2H_2S_2$)}$_2$] (**8**) into a mixture

Table 2
Selected crystallographic data of [{Ru(py$N_2H_2S_2$)}$_2$]Cl · 4MeOH ([**9**]Cl · 4MeOH) and [{Ru(py$N_2H_2S_2$)}$_2$](BF$_4$)$_2$ · 2DMSO · acetone · *n*-hexane ([**10**](BF$_4$)$_2$ · 2DMSO · acetone · *n*-hexane)

Compound	[**9**]Cl · 4MeOH	[**10**](BF$_4$)$_2$ · 2DMSO · acetone · *n*-hexane[a]
Formula	$C_{42}H_{50}ClN_6O_4Ru_2S_4$	$C_{51}H_{66}B_2F_8N_6O_3Ru_2S_4$
M_r (g mol^{-1})	1068.71	1379.22
Crystal size (mm)	0.50 × 0.40 × 0.30	0.40 × 0.38 × 0.30
F(0 0 0)	8720	2816
Crystal system	orthorhombic	monoclinic
Space group	*Fdd*$_2$	*C*$_2$/*c*
a (pm)	3036.2 (9)	2121.8 (4)
b (pm)	3574 (2)	1861.1 (4)
c (pm)	1659.3 (5)	1502.1 (3)
V (nm^{-3})	18.11 (1)	5.909 (2)
Z	16	4
ρ_{calc} (g cm^{-3})	1.577	1.550
μ (mm^{-1})	0.964	0.795
T (K)	298	200
θ Range (°)	1.76–27.01	2.8–52.0
Measured reflection	5815	7106
Unique reflection	5434	5814
R_{int}	0.0205	
Observed reflection	3881	3696
σ Criterion	$F_0 > 4.0\sigma(F)$	$F_0 > 4.0\sigma(F)$
Reflection parameters	540	356
R_1/wR_2	0.0415/0.0880	0.0894/0.2136
Absolute structure parameter [19]	0.05 (4)	

[a] Preliminary data.

of MeOH and CH_2Cl_2 (1:1) in the course of 48 h. Green single crystals of poor quality of [**10**]$(BF_4)_2 \cdot$ 2DMSO · acetone · *n*-hexane were grown by layering a solution of [**10**]$(BF_4)_2$ in DMSO/acetone (1/3) with *n*-hexane at −20 °C within one week.

Single crystals were sealed under N_2 in a glass capillary; data were collected either on a Nicolet R3m/V ([**9**]Cl · 4MeOH) or a Siemens P4 ([**10**]$(BF_4)_2 \cdot$ 2DMSO · acetone · *n*-hexane) diffractometer using Mo Kα radiation (λ = 71.073 pm, graphite monochromator). For [**10**]$(BF_4)_2$ · 2DMSO · acetone · *n*-hexane, an empirical absorption correction using XABS2 [17] has been performed, while for [**9**]Cl · 4MeOH absorption effects have been neglected. The structures were solved by direct methods and refined on F^2 using full-matrix least squares procedures (SHELXTL NT 5.10 [18]). Hydrogen atoms were geometrically positioned and allowed to ride on their carrier atoms with an isotropic displacement parameter fixed at 1.2 or 1.5 times Ueq of the proceeding C, N, or O atom. Table 2 lists selected crystallographic data. X-ray structure determination of [**10**]$(BF_4)_2 \cdot$ 2DMSO · acetone · *n*-hexane suffered from high residual electron density maxima localized in vicinity of the two Ru centers and probably disordered solvent molecules.

5. Supplementary material

Crystallographic data (excluding structure factors) for the structures reported in this paper have been deposited with the Cambridge Crystallographic Data Centre as Supplementary Publication Nos. CCDC 238306 and 238307. Copies of the data can be obtained free of charge on application to CCDC, 12 Union Road, Cambridge CB 21 EZ, UK (fax: +44 1223 336 033; e-mail: deposit @ccdc.cam.ac.uk or http://www.ccdc.cam.ac.uk).

Acknowledgments

We thank Professor Dr. Horst Kisch for his helpful suggestions. Financial support for this work by the Deutsche Forschungsgemeinschaft (SFB 583 ‘Redox-Active metal complexes’) and Fonds der Chemischen Industrie is gratefully acknowledged.

References

[1] (a) D.P. Mellor, in: F.P. Dwyer, D.P. Mellor (Eds.), Chelating Agents and Metal Chelates, Academic Press, New York, London, 1964, p. 44;
(b) K. Burger, in: K. Burger (Ed.), Biocoordination Chemistry, Ellis Horwood, New York, 1990, p. 11.
[2] (a) R.A. Henderson, G.J. Leigh, C.J. Picket, Adv. Inorg. Chem. Radiat. 27 (1983) 245;
(b) H. Kandler, C. Gauss, W. Bidell, S. Rosenberger, T. Bürgi, I.L. Eremenko, D. Veghini, O. Orama, P. Burger, H. Berke, J. Am. Chem. Soc. 110 (1988) 4872;
(c) J. Chatt, A.J. Pearman, R.L. Richards, J. Organomet. Chem. 101 (1975) 45.
[3] D. Sellmann, J. Utz, N. Blum, F.W. Heinemann, Coord. Chem. Rev. (1999) 607.
[4] D. Sellmann, J. Utz, F.W. Heinemann, Inorg. Chem. 38 (1999) 5314.
[5] (a) T. Tanase, K. Imagawa, S. Dev, Y. Mizobe, S. Yano, M. Hidai, New J. Chem. 12 (1988) 697;
(b) S. Dev, K. Imagawa, Y. Mizobe, G. Cheng, Y. Wakatsuki, H. Yamazaki, M. Hidai, Organometallics 8 (1989) 1232;
(c) H. Matsuzaka, Y. Hirayame, M. Nishio, Y. Mizobe, M. Hidai, Organometallics 12 (1993) 36;
(d) A. Takahashi, Y. Mizobe, H. Matsuzaka, S. Dev, M. Hidai, J. Organomet. Chem. 456 (1993) 243;
(e) K. Shiu, M. Chiang, S. Peng, G. Lee, J. Wang, L. Liou, Organometallics 17 (1998) 1790;
(f) H.K. Matsuzaka, Y. Mizobe, M. Nishio, M. Hidai, J. Chem. Soc., Chem. Commun. (1991) 1011;
(g) M. Nishio, H. Matsuzaka, Y. Mizobe, M. Hidai, J. Chem. Soc., Chem. Commun. (1993) 375;
(h) T. Kondo, S. Uenoyama, K. Fujita, T. Mitsudo, J. Am. Chem. Soc. 121 (1999) 482.
[6] (a) C. Sudha, S.K. Mandal, A.R. Chakravarty, Inorg. Chem. 33 (1994) 4878;
(b) E.P. Kelson, L.M. Henling, W.P. Schaefer, J.A. Labinger, J.E. Bercaw, Inorg. Chem. 32 (1993) 2863;
(c) A.R. Chakravarty, F.A. Cotton, M.P. Diebold, D.B. Lewis, W.J. Roth, J. Am. Chem. Soc. 108 (1986) 971.
[7] (a) F. Bottomley, Acc. Chem. Res. 11 (1978) 158;
(b) J.A. McCleverty, Chem. Rev. 79 (1979) 53.
[8] D. Sellmann, J. Utz, F.W. Heinemann, Inorg. Chem. 38 (1999) 459.
[9] D. Sellmann, J. Utz, F.W. Heinemann, Eur. J. Inorg. Chem. (1999) 341.
[10] B.R. Cameron, D.A. House, A. McAuley, J. Chem. Soc., Dalton Trans (1993) 1019.
[11] B.R. Cameron, G.J. Bridger, K.P. Maresca, J. Zubieta, Inorg. Chem. 39 (2000) 3928.
[12] T. Kondo, S. Uenoyama, K. Fujita, J. Am. Chem. Soc. 121 (1999) 482.
[13] (a) H.M. Koepp, H. Wendt, H. Strehlow, Z. Elektrochem. 64 (1960) 483;
(b) G. Gritzner, J. Kuta, Pure Appl. Chem. 56 (1984) 461.
[14] J.D. Gilbert, D. Rose, G. Wilkinson, J. Chem. Soc. (A) (1970) 2765.
[15] N.S. Al-Zamil, E.H.M. Evans, R.D. Gillard, D.W. Gams, T.E. Jenkins, R.J. Lancashire, P.A. Williams, Polyhedron 1 (1982) 525.
[16] J. Chatt, G.L. Leigh, A.P. Storace, J. Chem. Soc. (A) (1971) 1380.
[17] S. Parkin, B. Moezzi, H. Hope, J. Appl. Crystallogr. 28 (1995) 53.
[18] SHELXTL NT 5.10 Bruker AXS, Inc., Madison, WI, USA, 1998.
[19] H.D. Flade, Acta Crystallogr. (1983) 876.